2019

Mathematical Programming Approach for the Design of Satellite Power Systems

Allen Flath III
University of Kentucky, allenflath@gmail.com
Digital Object Identifier: https://doi.org/10.13023/etd.2019.126

STUDENT AGREEMENT:

I represent that my thesis or dissertation and abstract are my original work. Proper attribution has been given to all outside sources. I understand that I am solely responsible for obtaining any needed copyright permissions. I have obtained needed written permission statement(s) from the owner(s) of each third-party copyrighted matter to be included in my work, allowing electronic distribution (if such use is not permitted by the fair use doctrine) which will be submitted to UKnowledge as Additional File.

I hereby grant to The University of Kentucky and its agents the irrevocable, non-exclusive, and royalty-free license to archive and make accessible my work in whole or in part in all forms of media, now or hereafter known. I agree that the document mentioned above may be made available immediately for worldwide access unless an embargo applies.

I retain all other ownership rights to the copyright of my work. I also retain the right to use in future works (such as articles or books) all or part of my work. I understand that I am free to register the copyright to my work.

REVIEW, APPROVAL AND ACCEPTANCE

The document mentioned above has been reviewed and accepted by the student's advisor, on behalf of the advisory committee, and by the Director of Graduate Studies (DGS), on behalf of the program; we verify that this is the final, approved version of the student's thesis including all changes required by the advisory committee. The undersigned agree to abide by the statements above.

Allen Flath III, Student

Dr. Aaron Cramer, Major Professor

Dr. Aaron Cramer, Director of Graduate Studies

Mathematical Programming Approach for the Design of Satellite Power Systems

THESIS

A thesis submitted in partial fulfillment of the requirement for the degree of Master of Science in Electrical Engineering in the College of Engineering at the University of Kentucky

By

Allen Flath III

Lexington, Kentucky

Director: Dr. Aaron M. Cramer, Associate Professor of Electrical Engineering

Lexington, Kentucky

2019

ABSTRACT OF THESIS

Mathematical Programming Approach for the Design of Satellite Power Systems

Satellite power systems can be understood as islanded dc microgrids supplied by specialized and coordinated solar cell arrays augmented by electrochemical battery systems to handle high-power loads and periods of eclipse. The periodic availability of power, the limited capacity of batteries, and the dependence of all mission service on power consumption create a unique situation in which temporal power and energy scarcity exist. A multi-period model of an orbital satellite power system's performance over a mission's duration can be constructed. A modular power system architecture is used to characterize the system's constraints. Using mathematical programming, an optimization problem can be posed such that the optimal power and energy ratings for the power system are determined for any load schedule imposed by a given mission's requirements. The optimal energy trajectory of the electrical power system over a mission's duration is also determined when the mathematical programming problem is solved. A generic set of mission requirements is identified to test this approach, but the objective function of the resulting optimization problem can be modified to return different results. These results can provide a clear illustration of the trade-offs that designers of such power systems consider in the design process.

KEYWORDS: satellite power systems, mathematical model, distributed power generation, modular architectures, multi-period models,

Allen Flath III

April 16^{th}, 2019

Mathematical Programming Approach for the Design of Satellite Power Systems

By

Allen Flath III

Aaron M. Cramer
Director of Thesis

Aaron M. Cramer
Director of Graduate Studies

April 16^{th}, 2019
Date

I'd like to dedicate this work to all of the aspiring minds who seek to make science fiction a growing and positive reality, and all of those who support and inspire others to meet their craziest dreams.

Acknowledgements

I would like to acknowledge all of my professors and friends that welcomed, encouraged, and supported me during the last seven years attending the University of Kentucky. Particularly, my graduate advisor Dr. Aaron Cramer served as an invaluable mentor since I was a sophomore, and I have been entirely blessed to serve as his research supervisor for the last two years on the most interesting work I've had the pleasure of experiencing. My fraternity, Phi Gamma Delta, served as a crucial support structure and gave me many friends that I can count on to this day, in addition to inspiring me to be the best student and friend I could possibly be. My lovely fiancee (soon to be wife in a short handful of weeks!), has been by my side through many ups and downs and has never let me give up on any of my wildest dreams. Her ability to constantly put up with my bad jokes and pestering is truly the most inspiring testament of endurance that I could have in my life. Thank you and much love, Emily. Finally, nothing can compare to the everlasting impact my parents Al and Mary Flath have had on my life. I was lucky enough to learn almost all of what I know about honor, respect, and appreciation living under the same roof as these two. I have learned much more in my time away from home, but I was always able to use their influence on my life to direct myself to like-minded situations and opportunities that could teach me more than I thought possible.

Contents

List of Tables

List of Figures

Chapter 1

Introduction

A focus on small satellite spacecraft has supported low-cost, fast-fabrication platforms that have greatly expanded the capability of low-orbit space research missions [1] [2]. The spacecraft's power system and its control methodology are two crucial design aspects of such spacecraft. Any dedicated mission must have a platform capable of generating and delivering appropriate amounts of power throughout the satellite over the course of its service. The devices found in aerospace systems are generating and consuming power in increasingly complex ways in to achieve goals such as maximizing system performance, expanding mission capability, and improving survivability [1]. As such, the capabilities and the scope of missions these platforms have been utilized for has expanded far faster than the ability of system designers to compare competing platforms or device alternatives for their small satellites. Often, successful platforms from past missions or experiments are modified with instinct and intuition, tested for feasibility and then fine-tuned as needed, sometimes needing to be redesigned entirely. This can turn into a costly process with respect to material and man power even if the participating engineer has the best of intuitions regarding

his system's needs. Aerospace designers must have access to tools that will accurately and efficiently provide insightful metrics for power system design of aerospace systems.

Although this work will focus on the specific problem of nanosatellite power systems, the same problems exist on a larger scale when designing larger systems, and it is the hope that the methods and tools discussed herein can be extrapolated to larger systems with the appropriate considerations being taken. The difficulty of accurately illustrating the trade space when designing satellite power systems can potentially cost many hours of added time in the design process and thus creates a significant hurdle in producing an efficient fabrication process for any satellite power system. As the general process is improved with available tools and software, the discipline of aerospace design will also become more easily accessible from entry level participants. Small-satellites were initially developed to teach the principles of spacecraft design in an easily digestible manner, in addition to making this process more accessible to institutions that operate on a limited budget [3]. It is important to continue to address the initial desire for these platforms and the impact that improvements in the design process can have, despite their use in significant science missions and their expected adoption for ever more professional applications. As the efficiency of the design and development process of such systems improve, the total number of missions that can be undertaken will increase.

The scope of scientific space missions and studies is growing to include previously unthinkable situations and environments due to the reduced investment required for nanosatellite platforms [1]. Nanosatellites have gone from being exclusively used in the low-earth orbit (LEO) environment to assisting larger platforms in deep-space

missions [4], and they are widely being considered as ideal candidates for investigating and possibly prospecting asteroids and other small bodies [5] [6] [7] [8] [9]. Even in LEO environments. the problem of designing these systems is increasing as their applications are expanding to utilize higher-cost equipment on single platforms, and even swarms of multiple nanosatellites to achieve a single goal such as communication or fast-paced imaging of large areas. The design trade space imposed by harsh space environments, and the increased complexity of multi-platform systems, is not always clear or intuitive to navigate [10]. Though traditionally not expressed in these terms, the problem can be generalized to a matter of evaluating opportunity costs in the design process, or the loss of potential benefits from one chosen alternative when another alternative is chosen. Since the future can never be known with absolute certainty, opportunity costs are difficult to conceptualize, but some evaluation and comparison of an expected alternative must take place to determine the viability of one system over another. As the aerospace systems that will meet the space missions of today and tomorrow are being designed, improved concepts of evaluating and deciding between these increasingly complex opportunity costs will result in more effective systems when executing their planned missions, from executing simple technological demonstrations to highly sophisticated deep-space reconnaissance.

Previous experimental studies performed on the power systems of small satellite spacecraft have found that a distributed architecture provides unique opportunities to utilize a modular and flexible design approach, supporting the creation and implementation of reusable system designs and control protocols for missions of similar scope [11]. This distributed architecture can then be utilized in terms of the design problem. Instead of considering an exhaustively described and burdensome

system of equations where the power is generated from individually described solar cells, transferred across all necessary power conditioning, energy storage, and distribution infrastructure to meet the system's load demand, this distributed architecture breaks down the entirety of the satellite system into three different types of functional modules that together can describe the functionality of any spacecraft with respect to the power system, greatly simplifying the power analysis of any such system. This architecture is used in conjunction with a cost-minimizing design philosophy developed originally for naval shipboard power systems, in which mathematical programming is used to determine the optimal system topology that is capable of facilitating the optimal power flow of the system over the course of a mission [12]. This work will focus on optimizing the selection of components for a satellite power system instead of determining an optimal topology, as the topology of a small satellite power system is already pretty limited by the small and limiting form factor. Once a spacecraft's effective load demand has been approximated for its mission lifetime, the system can be expressed by an appropriate system of equations that dictate the system's behavior in the satellite's orbital environment. A set of equations can then be formed that predicts the behavior of the power system over the course of the satellite's mission. The design problem of selecting appropriately rated system components can then be posed as an optimization problem and mathematical programming can be used to solve for the desired ratings of specific system components, using constraints defined by the laws of conservation of energy and the expected behavior of the power system. In the case of the demonstrations presented herein, the system's acceptable minimum ratings for solar generation and battery capacity are found, and then expressed in terms of real life components using real life metrics that can easily be deduced from

component datasheets. This same process can be performed in the context of a number of environments and load profiles to see a clear illustration of the trade space that aerospace system designers experience. Considerations have also been taken to consider the impact of the hostile environment these systems are located, as the same load profile can be assessed for a satellite at the very beginning of its mission lifetime to the very end, with the relevant impact on the solar cell's performance from intense radiation exposure and the battery's reduced performance over time. Because the satellite power system's behavior must be determined over the course of its dedicated mission as a part of the optimization process, the optimized result also delivers an optimal schedule for the behavior of all components of the satellite power system. As will be discussed in more detail, this behavior is determined in such a way that it is not intuitive in regards to a traditional simulation approach that is typically hindered by the behavior of existing components that inspired the simulation, and the way traditional simulation tools handle timing. As such, the resulting power system behavior, hereafter referred to as the "energy trajectory", should also provide some insight into the design of actual control procedures. The end result is essentially a design tool that can inform every step of the satellite power system design process.

The remainder of this work is organized as follows. In chapter 2, a background of the technical aspects underpinning the design approach will be explored with a brief explanation of the advantages of the modularized architecture and mathematical programming. Chapter 2 will conclude with a brief literature review examining the relevant research surrounding and intersecting this work, the historical context of small satellite technology and the advent of the CubeSat standard, and illustrating the novelty this work contributes to the field. In chapter 3, the specific mathematical

programming approach will then be explained in detail, explaining the novel aspect of the design approach and the details of the specific mathematical program to be solved. Additional work that was performed to advance the design approach to an I/V level breakdown will also be shared. Chapter 4 will explore the different case studies that will help show the functional capabilities of the design tool, from minimizing the size or weight of a single system with specified component models, to illustrating the trade space when shifting the priority between a minimum size or weight system. Chapter 5 will share the results of these case studies with associated discussions regarding the impact of the findings. Finally, chapter 6 will briefly summarize the work and its conclusions, ending with a future outlook of work that can be performed to improve the design approach and its applications.

Chapter 2

Background & Literature Review

2.1 Background

2.1.1 Distributed Architecture

Naturally, smaller satellites contain simpler power systems and achieve less power-intensive mission objectives, simplifying the design process. The proposed design approach will leverage a modular electrical power system (EPS) architecture as presented in [11], which takes many concepts from distributed topologies while still leveraging some benefits of a centralized architecture. Distributed power system architectures are more common in more complex power systems, such as larger satellites and aircraft. There is typically a high voltage bus central to the system, and each subsystem that requires power is connected to the bus with an appropriate way to condition the power for use. The selected architecture is presented in Figure 1.

Distributed architectures have been used in aircraft with voltages from 28 to 270 VDC [13] [14]. Higher bus voltages implies lower currents to deliver the

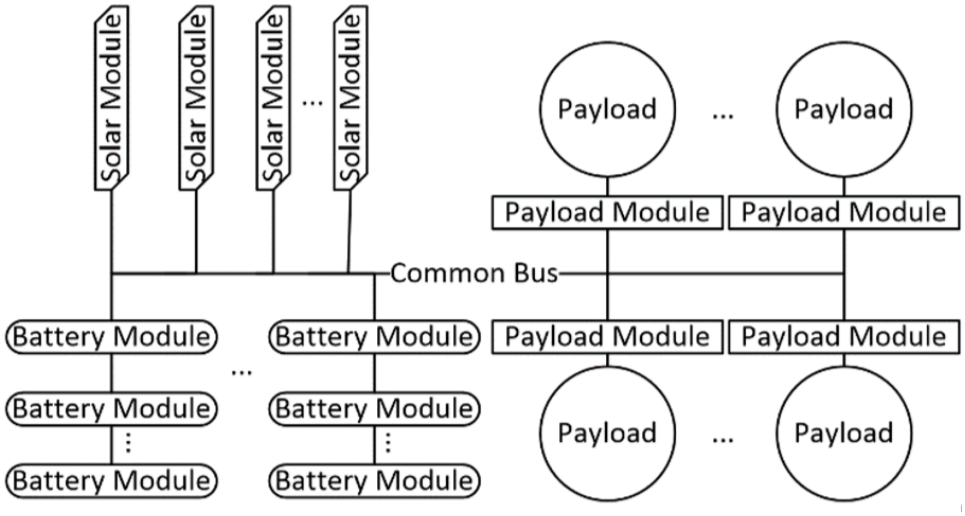

Figure 2.1: **Diagram of a Distributed Architecture [6].**

same amount of power, but this lower current being sent throughout the system can minimize energy loss and optimize efficiency due to less power being lost to heat and smaller eddy currents. Higher currents then intuitively implies more losses, and the higher system resistances required to safely handle these currents would also imply a higher material cost.

Any EPS using the chosen modular architecture can be separated into three different types of modules: solar modules, battery modules, and payload modules. Solar modules contain the solar panels used to generate power for the system. Battery modules contain the energy storage elements that will be responsible for storing excess power as energy, supplying excess power to high-demand loads, and function as the main sources of power when the solar modules are not generating power. Payload modules are for any type of dedicated energy usage, whether it be for housekeeping or mission loads. Every type of module also contains any power conditioning components that are necessary for that module to transfer energy to and/or from the bus.

The primary benefits of a distributed architecture are scalability and reusability, but they are also associated with higher efficiency and more resilient fault tolerance [13]. The distributed bus makes it so that any subsystem that needs power only needs an acceptable interface between the subsystem and the bus. Assuming that all necessary components have an appropriate connection to the bus, the only limitation on the number of attached subsystems is the total power available from the bus. Compared to a centralized architecture, the main limitation is the total power available from a regulator. This scalability can be leveraged to use one distributed topology for a wide variety of possible missions. Reusability is tied to scalability but it still provides unique benefits. Reusability implies that these subsystems can be readily used in any system that has a distributed bus for which it was designed. If a distributed bus is different from the one that a subsystem was originally designed for, only the interface needs to be redesigned. As such, subsystems from previous missions can be used in any combination as needed for future missions.

The efficiency improvements are desirable when compared to centralized competitors because the subsystem interface is designed entirely for the sake of the individual subsystems. Thus, the power conditioning and regulation circuits are typically designed for maximum efficiency under normal operation conditions. A centralized architecture's common regulator cannot operate at its designed optimal point if any of the subsystems being regulated are currently inoperable or inactive.

Fault-tolerance is a crucial aspect of any power system, but it becomes one of the most important design aspects when the system is impossible to reach for any kind of significant maintenance or repairs. Thus, a single fault could be the difference between a space science mission succeeding or drastically failing. Since

every subsystem is responsible for its own regulation in a distributed architecture, a single subsystem experiencing a fault or other anomaly is less likely to impact adjacent subsystems. If a subsystem draws too much current through its dedicated voltage regulator, other subsystems will likely be able to operate normally. In a centralized approach, an overloaded regulator would result in every subsystem connected to the common regulator experiencing a loss of service.

For all of the benefits a distributed architecture provides, there is of course a number of disadvantages that makes centralized architectures the primary choice for nanosatellite power systems. Extra circuitry is required to interface each individual subsystem to the bus to provide the dedicated regulation benefits discussed earlier. More circuitry and components usually implies more points of failure in an electronic system, which can over-all have a negative impact the crucial aspect of fault-tolerance. Of course, this circuitry and components will take up an increasingly significant amount of space as more subsystems are needed, eventually resulting in a loss of usable space that other subsystems could utilize to make a more capable system. Switching regulators necessary to interface the subsystems to a distributed bus can also increase the instability of a system [15] [16]. The last drawback is that, while a distributed architecture is scalable, there is more design work involved in creating an interface for each new subsystem to make it scalable. Not all missions or budgets will accommodate the extra time required to properly design the distributed power system.

2.1.2 Mathematical Programming

Mathematical programming is a form of optimization in which the best element (with regards to specified criteria) from some set of available alternatives is determined. In its simplest form, the maximum or minimum possible result of a real function is determined. It is possible to model the behavior of a satellite's EPS by determining the minimum cost of such a system when operating under nominal mission conditions. This formulation is subject to additional constraint equations to ensure the satisfaction of mission objectives, the conservation of energy, etc. Linear programming is a form of mathematical programming in which the requirements are expressed as linear relationships:

$$\begin{aligned} \underset{\mathbf{x}}{\text{maximize}} \quad & \mathbf{c^T x}, \\ \text{subject to} \quad & \mathbf{Ax} \leq \mathbf{b}, \\ & \mathbf{A_{eq} x} = \mathbf{b_{eq}}, \\ & \mathbf{x} \leq \mathbf{0}. \end{aligned} \tag{2.1}$$

The vector $\mathbf{x}$ contains the decision variables of the optimization problem. The vector $\mathbf{c}$ represents the weights of different variables in the objective function.

The matrix $\mathbf{A}$ and the vector $\mathbf{b}$ represent inequality constraints associated with the problem, and the matrix $\mathbf{A_{eq}}$ and the vector $\mathbf{b_{eq}}$ represent equality constraints.

2.2 Literature Review

2.2.1 Relevant Research in Area

Satellite power system design is typically approached by a multi-step process [17]. First, specific requirements of the system are identified, such as the average electrical power, the peak electrical power, the mission life, orbital parameters, and the spacecraft configuration required of the system. Second, an appropriately sized power source is selected that can fit the spacecraft's form factor to generate enough power for the satellite. Typically, this second step is defining the required sizing and configuration of a solar array. Third, an appropriate energy storage element is selected that can power the satellite during eclipse periods where power cannot be generated by the power source. Finally, appropriate power conditioning devices are selected to interface the power source, energy storage, and system loads to the power distribution system. The many derived requirements from each of these steps can easily impact previous design decisions, even the decisions made in the previous step. This can force designers into lengthy iterated design processes. Recent efforts have been undertaken to formulate a CubeSat model-based system engineering reference design [18], the goal of which is a baseline design for a typically desired CubeSat, which can then be specifically modified to meet specific mission requirements as needed. A logical next step would be the development of effective methods and tools to help determine the appropriate modifications to the reference design to meet specific mission requirements. These do not need to specifically be applicable to CubeSats, or even tied to the base model, but the use of such a base model will probably improve the design

experience. An example of such work seeking to optimize the design of a CubeSat reference model with given component alternatives is given in [19], which uses a genetic algorithm to analyze the trade-offs involved in designing the power supply system of a low-earth orbit spacecraft.

Typically, improvement of the satellite design process involves modifying the typical equations and steps found in the process illustrated in [17] and simulating in different operational environments to see if the improvements are feasible, or in need of more tweaking [20]. Work has also been performed to formulate a flexible controller design for satellite electrical power systems for CubeSats varying from 1U (a singular CubeSat) to 12U (12 CubeSat models integrated into a single platform) [21], which can provide a useful standard to analyze the byproduct of the design tool discussed herein. Of course, these theoretical control methods usually cannot predict how the system actually behaves in real life. Work has been done to design a power system with advanced telemetry capability that actually determines the real-time efficiency of a satellite CubeSat power system and observes the impact that undesirable environments and situations can have, to formulate a proper system response to maintain efficient behavior [22]. Studies analyzing potential missions are also crucial to the viability of this research, as any feasible mission where a small satellite can be used is a potential application for the tool. A study such as [23] observes the feasibility of different methods for coordinating propulsion of swarms of spacecraft and can both utilize the tool discussed in this work, and open potential doors for its use.

2.2.2 Historical Context

Small satellites have been in use since 1986, when the Soviet Union launched 24 microsatellites as a military communications constellation. All of these satellites weighed over 60 kg, had an expected lifetime of around 2 years, and provided medium-range, record-and-forward communications within the low-earth orbit environment. In 1970, these same models of microsatellites were launched 8-at-a-time using boosters. Between 1970 and 1993, 30 operational satellites were providing fairly complete coverage of the earth using randomly distributed signals at any given time. A major enabling event for small satellite technology occurred when the Soviet Union fell, and all progress spent developing intercontinental ballistic missiles now left a marketable product that was widely available to the world for low-cost launch vehicles. This opened the doors for the first large LEO commercial communications constellations to be established throughout the 1990's [24].

NASA's CubeSat program was conceived in 1999 as a tool to help teach students and fledgling aerospace engineers about the process of developing, launching, and operating a spacecraft. Every major aspect of a spacecraft's life cycle can be studied by the production of a CubeSat, so the goal was to give students an opportunity to "learn-by-doing" on a small, but still significant scale to produce competent graduates right out of school. The CubeSat standard was developed as the first step to provide basic physical features and safety requirements for potential developers [25]. Today, standard CubeSats are 10x10x10 cm and weigh no more than 1.3 kg per unit (making them classifiable as picosatellites) and have lifetimes that can span up to 4 years.

2.2.3 Context for Novelty

The novelty of this work is found in the method of determining the minimum system performance required to accomplish mission objectives, which is then processed into a minimized system. The multi-period approach of determining the power system's optimal behavior, which will be further explained in Ch. 3, does not rely on any heuristic models or a hard-coded ruleset. It instead focuses on determining the optimal behavior over an entire mission with nothing but a set of constraints dictating the laws of physics and the limits of the individual component modules. Optimization techniques have been used in the design and modeling of individual power system components, such as power converters [26], and general power allocation in a real-time simulation [27] but this method of optimization has only been used in context of controlling naval shipboard power systems. It is worth noting that while this method has been used for the control of those systems, the design and functional capacity of the components in the system were already determined, whereas this approach seeks to design the satellite power system as a consequence of the optimized energy trajectory for the chosen satellite mission.

Chapter 3

Mathematical Programming Approach

3.1 Single-Period vs. Multi-Period Modeling

The time duration of the problem is arbitrary. The design approach can be used to solve for the optimal design of the system when considering a single second start-up, up to an entire satellite's expected lifetime. A single orbital period will be used for simplicity in following demonstrations.

A time-step, ΔT, is defined as the time (in seconds) elapsed between each point of time being considered in the optimization problem. The time-step can be increased to improve run-time, or decreased to improve the resolution of the solution. Due to the discrete nature of the approach, it is possible that time-steps that are inappropriately large will cause the solution to appear incorrect. Imagine a one-minute mission with 20 second time-steps, and a mission load turning on at 30 seconds. When solved, the load turning on would not become apparent until the point occurring at 40 seconds,

imposing what appears to be a 10 second delay in the load's proper operation, when the correct time to turn on the load was simply not being considered. Thus, proper care must be taken in analyzing the results when this kind of behavior is expected.

An optimal energy trajectory for an EPS over the course of a satellite mission is intuitively time-dependent, since any mission will have objectives to accomplish within specified windows of time. Thinking again about opportunity cost, it is reasonable to assume that the energy storage module should decide to store energy in two cases: when future load demands require more power than the generation module can supply, and when the battery does not have enough energy stored to survive the next eclipse period. The generally unintuitive part is determining the optimal time to store this energy.

When evaluating the problem, the behavior of the system can be determined over time in one of two ways. The energy trajectory can be optimized in terms of one moment to the next moment, or optimized with respect to the desired behavior of the system over the course of the entire mission. The former approach would involve evaluating the optimization problem as every time step is processed, only taking into account the variables, parameters, and mission objectives imposed at the beginning of the time step to best meet the desired mission objectives at the end of the time step. For example, if the spacecraft must operate an on-board camera 30 seconds into the mission with a 1 second time step, it would not be able to begin to meet the power demand of the camera, and the associated impact on the battery's behavior, until the 29th second. This approach more accurately mirrors the operation of a real-life control system dictating the actions of a spacecraft, but there is no guarantee that this approach delivers a truly optimal energy trajectory that the spacecraft could possibly

take. While this is a more accurate way to represent a real-life control element, this is a fundamental limitation to the design problem. A more effective design solution is possible when allowing the evaluation of the optimization problem to consider the expected possible future of the spacecraft's power system [28]. A larger system of equations can be formulated to constrain the optimization problem, with one set of equations for the system representing every time step that the spacecraft is expected to service. With this approach, the mathematical programming problem can consider unintuitive cases where the system is allowed to prepare for the future burden that the system load and eclipse periods will impose on the system. Borrowing again from the example above, the system can now evaluate the optimal time to make adjustments to the system at any moment leading up to the 30th second. The result is the optimal energy trajectory when considering the entire lifetime of the satellite, and thus the true optimal power ratings of the system components can be determined. Of course, there is the question of how applicable this result will be in terms of designing real-life systems that experience the limitations of real-life control elements, but this can become a moot point with the advancement of power system control schemes that seek to alleviate these limitations, such as those explored in [28].

3.2 Power-Flow Level Approach

For any system to be feasible, the power demands of the described loads must be satisfied by the power system comprised of the power source and storage elements. The first goal of this work is to develop a tool that can quickly and accurately illustrate and navigate the trade space faced by satellite power system designers. This tool

doesn't have to necessarily choose the system that will be sent to fabrication, but it will definitely be able to overrule a number of designs that could be wasted in fabrication.

3.2.1 Decision Variables

The design problem presented herein has five types of decision variables that describe the behavior and design of the power system. Three of the decision variables are tied to behavior of the system at any given second, and thus there are a set of these three decision variables for every time-step being considered by the problem. These are the output of the solar generation module, $P_{pv,i}$, the output power of the battery module, $P_{B,i}$, and the energy currently stored in the battery, $E_{B,i}$, where i represents the time-step associated with each variable. All units of power and energy are expressed in terms of W and Wh, respectively.

The other two decision variables are global decision variables that describe the design of the power system, and do not change over time like the other decision variables. These are the maximum power rating of the solar generation module, P_{pvmax}, and the maximum energy capacity of the battery, E_{Bmax}.

3.2.2 Constraints

Any LEO orbit will take the satellite through alternating periods of direct sunlight exposure and of eclipse. For the purpose of this work, solar power generation is not possible during periods of eclipse. Though there could be incidental irradiation reflected from surrounding bodies, this is not a reliable source for solar power

generation and is largely negligible when compared to the overall performance of the satellite's EPS. The total orbital period experienced by a satellite can be found by

$$T = \frac{2\pi}{\sqrt{\frac{\mu}{R^3}}}, \tag{3.1}$$

where μ is the standard gravitational parameter of $3.986 \times 10^{14} \frac{\mathrm{m}^3}{\mathrm{s}^2}$ and R is the orbit's effective radius. The effective radius is equal to the radius of the body, r, added to the altitude of the satellite, a. The orbital period is separable into periods of sunlight and eclipse according to the eclipse fraction, which can be found according to

$$f_e = \frac{1}{\pi} \arccos \frac{\sqrt{a^2 + 2ra}}{R \cos \beta}, \tag{3.2}$$

where β is the beta angle. The beta angle can vary between $+90$ and -90 degrees and is an expression of how long an orbital spacecraft will spend in sunlight. Once the eclipse fraction is determined, it can be used to calculate the amount of time the spacecraft will spend with no solar generation.

The one-bus distributed architecture shown in Figure 1 has a system of equations that constrains the flow of power and energy throughout the system. The power needed by the payload module in the current moment i, $P_{L,i}$, must be provided by the power supplied from the generation and battery modules in the same moment,

$$P_{L,i} = P_{pv,i} + P_{B,i}. \tag{3.3}$$

The generation module cannot provide negative power and cannot provide more power than the current orbital environment allows, represented by a proportional constant $\alpha_i \in [0, 1]$, that is determined by the orbital environment of the satellite. The maximum rating of the pv module, $P_{pv,max}$ limits the power output when the orbital environment allows for full generation,

$$0 \leq P_{pv,i} \leq \alpha_i P_{pv,max}, \tag{3.4}$$

The battery module cannot contain negative energy or more energy than the maximum rating allows, enforced by,

$$0 \leq E_{B,i} \leq E_{B,max}. \tag{3.5}$$

The battery module cannot charge or discharge energy faster than the charging and discharging rates that the style of battery dictates, which is limited by the current energy capacity of the battery by,

$$-\gamma_c E_{Bmax} \leq P_{B,i} \leq \gamma_d E_{Bmax}. \tag{3.6}$$

The energy of the battery at $i+1$ is the energy supplied by the battery in the last time step, Δt, subtracted from the energy contained in the battery at i, $E_{B,i}$,

$$E_{B,i+1} = E_{B,i} - \Delta t P_{B,i}. \tag{3.7}$$

This is the intertemporal constraint that "moves the problem forward" by solving for a variable in the next time-step, $i+1$. Of course, the last time-step, N, of

the problem also needs to satisfy this equation, and this is done by using the original state of the battery at the beginning of the problem in place of $E_{B,i+1}$. This ensures a cyclical nature of the solution. Simply put, at the last time-step of the problem to consider, Eq. 8 becomes:

$$E_{B,1} = E_{B,N} - \Delta t P_{B,N}. \tag{3.8}$$

3.2.3 Weights

There are costs associated with having a unit of generation capability and a unit of energy storage capability installed in the system, c_{pv} and c_B. Real life components and devices can be assessed to determine an appropriate selection for the system costs. If the system mass is being minimized, the expected specific energy (in terms of kg/W or kg/Wh) of components can be determined to give the solver an accurate measure of how much to penalize each associated decision variable.

3.2.4 Power-Flow Level Programming Problem

Once a schedule for the power demand of the satellite over the course of a mission is determined, all of the presented decision variables, constraints, and weights, can be assembled to formulate a linear programming problem of the following form:

$$\begin{aligned} \underset{P_{pvmax},\, E_{Bmax}}{\text{minimize}} \quad & c_{pv}P_{pvmax} + c_B E_{Bmax} \\ \text{subject to} \quad & \mathbf{Ax} \leq \mathbf{b}, \\ & \mathbf{A_{eq}x} = \mathbf{b_{eq}}, \\ & \mathbf{x} \leq \mathbf{0}. \end{aligned} \tag{3.9}$$

After performing the optimization, the minimum system requirements, and the optimal path of control of the system over the simulated mission are determined. Using specific real-life components that informed the selection of the system costs, these results can be used to determine the necessary surface area of the solar panels and the mass of the battery to meet these minimum requirements.

3.3 I/V Level Approach

With a fully described set of equations to express any modularized satellite power system with power flows, it is possible to identify feasible and unfeasible system designs in terms of the over-all power demands of the system. However, these power flows do not just magically arise when requested - there are real world voltages and currents being monitored and regulated to deliver the necessary power throughout the system. A more realistic approach would be to break down the system's behavior to the actual currents and voltages throughout the power system that we are concerned with. This could provide designers with the ability to trouble-shoot individual modules in addition to improving the accuracy of the illustration and navigation of the trade space.

A significant problem arises when considering the necessary equations to accomplish this. Almost all of the required decision variables are not in linear relationships, and most of them are tied to each other with no possibility of isolating them. It is possible to address this in two ways: turn to a form of non-linear mathematical programming, or linearize the equations so it can still be solved with linear programming. Both approaches have their drawbacks. Non-linear programming requires much more computation effort to solve problems, which themselves take more and sometimes very complicated steps to pose to a solver. Linearizing the equations requires handling a heavy load of partial derivatives to express the impact of changing each individual variable on the output. These derivatives would remain constant with respect to each individual time step, resulting in linear equations that will still be quickly solved by a linear programming optimizer, but at an unavoidable cost to the accuracy of the result. Both approaches would require much more information from the system components being documented and processed, and the approaches would likely have to be completely reformulated for any component that does not behave in the typical nature described herein, possibly increasing the front-end work load of using this design approach to the point of being counter-productive, but this would be off-set for system templates that see enough widespread and repeated use.

For the sake of minimizing the computation time for using such a tool, a linearization process following methods in [29] and [30] is chosen to describe a set of approximated equations. This was not able to be completed with any meaningful results for reasons that will be discussed, but this still represents a large portion of work that went into this design approach and only a few steps, though they are rather large, would be necessary to complete this level of resolution for the tool in the future.

3.3.1 Decision Variables

The flow of power will still be the same as it was before, but now it depends on different voltage and current variables to propagate the power, and so the decision variables that were necessary for every time-step will change. For this work they are the voltage of the central bus at a given time-step, $V_{bus,i}$, and the state of charge of the battery at a given time-step, SOC_i, which is a proportional constant between 0 and 1 describing the remaining charge in the battery. As before, there is a set of each of these decision variables for every time-step that that is to be optimized. These decision variables may also change if a different approach to linearization is taken than the one used herein.

In order to properly express the construction of a system in terms of voltages and currents, the individual modules must be characterized and enumerated. Whereas before, the power-flow level tool was deciding the size of a single solar module, now the I/V level tool will define the performance of a single characterized module and determine how many modules are required. This could return non-integer answers, but of course the answer need only be rounded up for each type of PV and battery module to meet the minimum requirements of the power system. Furthermore, these modules can be placed in series or parallel with each other, so each module will have two design variables representing the number of modules in series and in parallel, respectively. Assuming that n represents series, and m represents parallel, then we have four decision variables to add to the rest. They are: the number of solar modules in series,n_{pv}, the number of solar modules in parallel, m_{pv}, the number of battery modules in series, n_{batt}, and the number of battery modules in parallel, m_{batt}.

3.3.2 Constraints

The exact same orbital constraints that applied to the power-flow level analysis are still relevant here. In fact, the main power constraint represented in Eq.3.3 is still the main constraint being enforced for this version of the programming problem. However, to express this equation at the I/V level, this equation needs to be broken down into the different elements of $P_{pv,i}$ and $P_{B,i}$. Furthermore, these no longer represent the power of individual modules that could theoretically be an arbitrary size, but the total sum of power from a collection of predefined sized modules. First, the power of the solar modules will be defined followed by the power of the battery modules. The power of the solar modules is defined as the current out of the solar modules times the bus voltage,

$$P_{pv,i} = V_{bus,i} I_{pv,i}. \tag{3.10}$$

The current out of the solar modules, I_{pv}, can be defined as such:

$$I_{pv,i} = \alpha_i I_L - I_0[e^{\frac{\frac{V_{bus,i}}{m_{pv}} + R_s \frac{I_{pv,i}}{m_{pv}}}{\eta V_t}} - 1] - \frac{\frac{V_{bus,i}}{m_{pv}} + R_s \frac{I_{pv,i}}{m_{pv}}}{R_p - \frac{I_{pv,i}}{m_{pv}}}, \tag{3.11}$$

which shows the standard solar cell current equation accounting for the number of solar cells in parallel and in series. α_i is still the current solar availability at the given time-step which now limits the light generated current. R_p and R_s are the shunt and series resistances of the solar cell, which are sometimes given in the available datasheet, but can almost always be ascertained using the method found in [31]. The remaining terms are η, the diode ideality factor which is not always apparent, and

V_t, the thermal voltage. This equation is not only highly non-linear, but it is self referential, making the linearization even more difficult. However, this equation is of no use to a linear programming tool until it is linearized.

The power of the battery is defined as the voltage of the bus times the current out of the battery,

$$P_{B,i} = V_{bus,i} I_{batt,i}. \tag{3.12}$$

It is clear that the power of the battery is dependant on one of our decision variables, and I_{batt} can accurately be used as a placeholder for the following equation:

$$I_{batt,i} = n_{batt} \frac{V_{batt} - \frac{V_{bus,i}}{m_{batt}}}{R_{batt}}, \tag{3.13}$$

which shows the current from the batteries as a relationship between the bus voltage and the equivalent battery voltages, accounting for the impact of the possible series and parallel connections between multiple modules. R_{batt} is the resistance of the battery modules, which can be reasonably estimated from referencing a datasheet. V_{batt} is itself a nonlinear relationship dependent on the current state of charge, another one of our decision variables. There is no set equation for this and the relationship will change over the lifetime of the batteries, but the profile can be empirically observed and linearized for each unique battery chemistry. As mentioned before, the $P_{B,i}$ equation is obviously very nonlinear and decision variables are tied to each other. As such, this equation isn't of much use to us until it is linearized. It is still possible to describe how the state-of-charge changes from one time-step to the next,

$$SOC_{i+1} = SOC_i - \Delta t I_{batt,i}. \tag{3.14}$$

This equation is meant to connect the constraints from one time-step to the next and simulate the concept of a system reacting to the changing environment over time, just as the battery energy equation did for the power-flow level breakdown.

Between the total power equation and the SOC equation, it is not yet enough to accurately describe the behavior of the system. There is still highly non-linear behavior of the diode in any given solar cell configuration that was not able to be accounted for in this work. However, the presented equations still need to be adequately linearized to be of any use for future work where the constraints of this system are accurately described for the I/V level breakdown of the system.

Linearization of Constraints

To linearize each of the necessary equations, the variables to linearize must be chosen, as well as a representative value to linearize the equation with respect to each variable. For each of these representative values, as well as the standard constants associated with each equation, a reference configuration such as the one used in [11] can be addressed. First, the battery will be linearized, beginning with the battery power equation linearized about four variables: n_{batt}, m_{batt}, V_{bus}, and SOC. Partial derivatives must be taken with respect to each variable, and they are:

$$\frac{\delta P_{batt}}{\delta n_{batt}} = \frac{V^*_{bus}(V^*_{batt} - \frac{V^*_{bus}}{m^*_{batt}})}{R_{batt}}, \tag{3.15}$$

$$\frac{\delta P_{batt}}{\delta m_{batt}} = \frac{V^{*2}_{bus} n^*_{batt}}{R_{batt} m^{*2}_{batt}}, \tag{3.16}$$

$$\frac{\delta P_{batt}}{\delta V_{bus}} = -\frac{n^*_{batt}(2V^*_{bus} - V^*_{batt} m^*_{batt})}{R_{batt} m^*_{batt}}, \tag{3.17}$$

and

$$\frac{\delta P_{batt}}{\delta SOC} = \frac{V^*_{bus}\frac{dV^*_{batt}}{dSOC^*}n^*_{batt}}{R_{batt}}, \tag{3.18}$$

where any of the decision variables accented by an asterisk is a representative value around which we are linearizing. Non-decision variables accented by a star are a nominal value from the configuration. One thing that still stands out is the derivative in Eq.3.27, which is based on another linearization of the relationship between a polymer lithium-ion battery's voltage and its state-of-charge, performed in [32] and presented as:

$$V_{batt} = 3.3746 + 0.7604SOC. \tag{3.19}$$

The next step is to find a nominal value for P_{batt} that can then be used to infer the constant portion of the linearization. This is done by substituting the nominal values for the decision variables into the normal equation:

$$P^*_{batt} = -\frac{V^*_{bus}n^*_{batt}(V^*_{batt} - \frac{V^*_{bus}}{m^*_{batt}})}{R_{batt}}. \tag{3.20}$$

All of these pieces are then placed into an equation to find the constant portion of the linearization:

$$P_{batt0} = P^*_{batt} - \frac{\delta P_{batt}}{\delta n_{batt}}n^*_{batt} - \frac{\delta P_{batt}}{\delta m_{batt}}m^*_{batt} - \frac{\delta P_{batt}}{\delta V_{bus}}V^*_{bus} - \frac{\delta P_{batt}}{\delta SOC}SOC^*. \tag{3.21}$$

Everything is substituted into this equation to get a simplified equation much like the other parts:

$$P_{batt0} = -\frac{V^*_{bus} n^*_{batt} (V^*_{batt} m^*_{batt} - V^*_{bus} + SOC^* \frac{dV^*_{batt}}{dSOC^*} m^*_{batt})}{R_{batt} m^*_{batt}}. \tag{3.22}$$

The linear approximation for P_{batt} is finally given as

$$P_{batt} \approx P_{batt0} + \frac{\delta P_{batt}}{\delta n_{batt}} n^*_{batt} + \frac{\delta P_{batt}}{\delta m_{batt}} m^*_{batt} + \frac{\delta P_{batt}}{\delta V_{bus}} V^*_{bus} + \frac{\delta P_{batt}}{\delta SOC} SOC, \tag{3.23}$$

where everything but the decision variables are constants based off of an existing model, and thus can be used in a linear program to be quickly evaluated.

A similar process is performed to linearize the equation for the current from the battery, which is essential to update the state of charge of the batteries. First, the relevant derivatives are taken, linearizing about the same four variables:

$$\frac{\delta I_{batt}}{\delta n_{batt}} = \frac{V^*_{batt} - \frac{V^*_{bus}}{m^*_{batt}}}{R_{batt}}, \tag{3.24}$$

$$\frac{\delta I_{batt}}{\delta m_{batt}} = \frac{V^*_{bus} n^*_{batt}}{R_{batt} m^{*2}_{batt}}, \tag{3.25}$$

$$\frac{\delta I_{batt}}{\delta V_{bus}} = -\frac{n^*_{batt}}{R_{batt} m^*_{batt}}, \tag{3.26}$$

and

$$\frac{\delta I_{batt}}{\delta SOC} = \frac{\frac{dV^*_{batt}}{dSOC^*} n^*_{batt}}{R_{batt}}. \tag{3.27}$$

Then, the nominal value for I_{batt} is found:

$$I^*_{batt} = \frac{n^*_{batt} (V^*_{batt} - \frac{V^*_{bus}}{m^*_{batt}})}{R_{batt}}. \tag{3.28}$$

Still following the same process, the simplified constant portion is determined to be:

$$I_{batt0} = -\frac{SOC^* \frac{dV^*_{batt}}{dSOC^*} n^*_{batt}}{R_{batt}}. \tag{3.29}$$

This results in a finalized linear approximation for the current from the battery to be:

$$I_{batt} \approx I_{batt0} + \frac{\delta I_{batt}}{\delta n_{batt}} n^*_{batt} + \frac{\delta I_{batt}}{\delta m_{batt}} m^*_{batt} + \frac{\delta I_{batt}}{\delta V_{bus}} V_{bus} + \frac{\delta I_{batt}}{\delta SOC} SOC. \tag{3.30}$$

To begin linearizing the solar panels, the current equation cannot be self-referential, so a new function shall be defined where the term on the right is subtracted from both sides, like so:

$$g = 0 = \alpha_i I_L - I_0[e^{\frac{\frac{V_{bus,i}}{m_{pv}} + R_s \frac{I_{pv,i}}{m_{pv}}}{\eta V_t}} - 1] - \frac{\frac{V_{bus,i}}{m_{pv}} + R_s \frac{I_{pv,i}}{m_{pv}}}{R_p - \frac{I_{pv,i}}{m_{pv}}} - I_{pv,i}. \tag{3.31}$$

Next, this equation must be linearized about n_{pv}, m_{pv}, V_{bus}, and P_{pv}. Unfortunately, the pieces that make up the approximation are much too large to show on paper. It is essentially the same process that the battery entailed, but many more nominal values are required than before. The final results are also very similar to the battery linearizations, resulting in two approximations for the current and the resulting power from the solar cells:

$$g \approx g^* + \frac{\delta g}{\delta n_{pv}} n_{pv} + \frac{\delta g}{\delta m_{pv}} m_{pv} + \frac{\delta g}{\delta V_{bus}} V_{bus} + \frac{\delta g}{\delta P_{pv}} P_{pv}, \tag{3.32}$$

and

$$P_{pv} \approx P_{pv}^{*} + \frac{\delta P_{pv}}{\delta n_{pv}} n_{pv} + \frac{\delta P_{pv}}{\delta m_{pv}} m_{pv} + \frac{\delta P_{pv}}{\delta V_{bus}} V_{bus}. \tag{3.33}$$

3.3.3 Weights

For the weights to be accurately referenced in a solver, they must be applied appropriately reflect the possibility of adding modules in series and parallel. This is done similarly for both battery and solar modules:

$$C_{pv-IV} = n_{pv} m_{pv} c_{pv}, \tag{3.34}$$

and

$$C_{batt-IV} = n_{batt} m_{batt} c_{batt}. \tag{3.35}$$

These are not linear costs, and thus must also be linearized by a similar process to the constraint equations.

Linearization of Weights

There are only two variables besides the cost constant in each cost equation, and so they are the ones to linearize about. The four necessary derivatives are taken as:

$$\frac{\delta C_{pv-IV}}{\delta n_{pv}} = c_{pv} m_{pv}^{*}, \tag{3.36}$$

$$\frac{\delta C_{pv-IV}}{\delta m_{pv}} = c_{pv} n_{pv}^{*}, \tag{3.37}$$

$$\frac{\delta C_{batt-IV}}{\delta n_{batt}} = c_{batt} m_{batt}^{*}, \tag{3.38}$$

and

$$\frac{\delta C_{batt-IV}}{\delta m_{batt}} = c_{batt} n^*_{batt}. \tag{3.39}$$

The normalized values for both costs are:

$$C^*_{pv-IV} = n^*_{pv} m^*_{pv} c_{pv}, \tag{3.40}$$

and

$$C^*_{batt-IV} = n^*_{batt} m^*_{batt} c_{batt}. \tag{3.41}$$

Constant portions for each linearization are simplified to:

$$C_{batt-IV0} = -c_{batt} m^*_{batt} n^*_{batt}, \tag{3.42}$$

and

$$C_{pv-IV0} = -c_{pv} m^*_{pv} n^*_{pv}. \tag{3.43}$$

All of these pieces combine to the final approximations for the weights:

$$C_{batt-IV} = C_{batt-IV0} + \frac{\delta C_{batt-IV}}{\delta n_{batt}} n_{batt} + \frac{\delta C_{batt-IV}}{\delta m_{batt}} m_{batt}, \tag{3.44}$$

and

$$C_{pv-IV} = C_{pv-IV0} + \frac{\delta C_{pv-IV}}{\delta n_{pv}} n_{pv} + \frac{\delta C_{pv-IV}}{\delta m_{pv}} m_{pv}, \tag{3.45}$$

Chapter 4

Case Studies

4.1 Sample Mission Profile

The example environment is inspired by [33], a 650-km orbit around the earth with a period of 97.73 minutes, approximated as 99 minutes for the following demonstrations. This provides for roughly 63 minutes of sunlight exposure and 36 minutes of eclipse in a single cycle. Because generation is handled by solar panels attached to the spacecraft, the generation module's output power is going to fluctuate between

Table 4.1: **Mission Profile**

Subsystem	**Function**	**Load (W)**	**Working Period**
Communication	Beacon	0.25	Full Period
	Receiver	0.2	Full Period
	Transmitter	1.7	10 min
Mission	Camera	0.36	5 min
On-Board Computer	Processing	0.22	Full Period
Power System	Conditioning	0.25	Full Period
	Generation	0.05	Sunlight

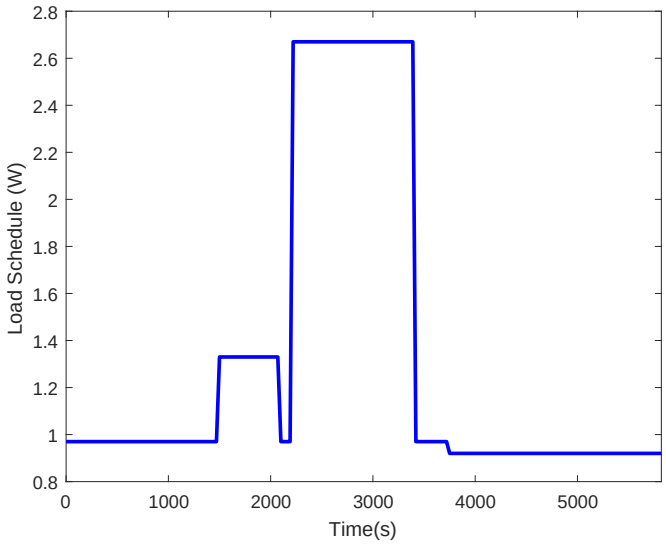

Figure 4.1: **Load Schedule**

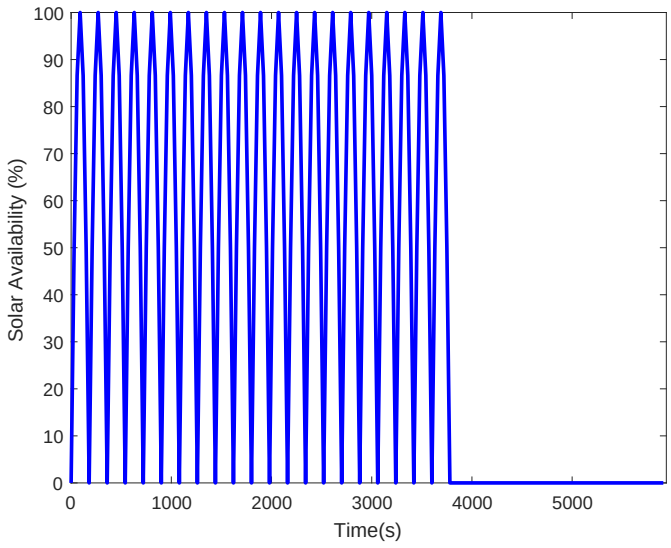

Figure 4.2: **Solar Availability Schedule**

its minimum and maximum value in a sinusoidal pattern. It is assumed that the solar generation is handled by two equally sized solar panels on opposite sides of the spacecraft, with an ideal rotational spin. This sinusoidal pattern is only positive, as if taking the absolute value of the sinusoid. The battery of the system will begin fully uncharged. The selected spacecraft will have a dedicated mission similar to the one defined in [34], with relevant details listed in table 4.1. Generally, the system will have a communications system, a typical camera to gather mission-relevant data, and an onboard computer system that all have load requirements over the course of a typical revolution. The system is expected to operate the camera for a five-minute period once during the solar period followed by a brief pause. Then, the system executes a relatively high-power transmission of the collected data over a period of ten minutes. Aside from the camera and the transmitter that only need to operate for a brief amount of time in each revolution, the satellite is constantly monitoring for incoming communications and operating a communications beacon to help receive those communications, in addition to the on-board computer and other house-keeping loads. The power system requires 0.05 less watts to operate during periods of eclipse. The schedules for the system load, $P_{L,i}$, and solar irradiance, α_i, are presented in figures 4.1 and 4.2, respectively.

4.2 Evaluating Minimum-Cost Systems Given Specific Components

The first and most obvious step to show the functionality of the design approach is to select the optimal power rating of the solar module and the energy ca-

pacity of the battery module when the real-life components are already selected. The components used in [11] are selected for the first study. Certain cost metrics, such as the amount of power the solar cells can deliver per gram or cubic centimeter, and the amount of energy the batteries can store per gram or cubic centimeter, must be determined according to each component being evaluated by the tool. No inefficiencies are considered. Trisol-X Solar Wings are selected for the solar-panels of the generation module, which have a specific power of 5.15 g/W, and a power density of 0.612 cm^3/W. Because the assumed generation system will ever only have half of the solar panels irradiated over the course of the system's rotation, the associated mass and volume costs are doubled throughout the rest of the calculations. Model PL544792-2C Li-Polymer batteries from BatterySpace are chosen for the battery module, which have a specific energy of 5.02 g/Wh, an energy density of 3.8 $\times 10^{-4}$ cm^3/Wh, a maximum charge rate of 0.50 W/Wh, and a maximum discharge rate of 2.02 W/Wh. Power lost to energy conversion and transfer across the system is ignored.

4.3 Evaluating Minimum-Cost Systems Given Component Alternatives

The next step to show what this approach is capable of is to give the tool a set of many different choices for the solar panels and the batteries. Of course, one could do this with any number of candidate components, but this study will limit it to five candidates for both of the solar and battery modules. Many solar cells are referenced in [20], but unfortunately no suitable datasheet was available for the clydespace solar cells, so Endurosat solar cells are used in their place. The reference configuration ex-

Table 4.2: **Associated Costs for Battery Alternatives**

Components	Specific Energy ($\times 10^{-6} kg/J$)	Energy Density ($\times 10^{-10} m^3/J$)
Polymer Li-ion	1.40	7.31
Ni-Cd	1.94	10.52
Ni Metal Hydride	3.18	9.92
Li-ion	2.80	8.01
LiNiMnCo	1.95	29.68

Table 4.3: **Discharge/Charge Rates Per Capacity for Battery Alternatives**

Components	Discharge Rate ($\times 10^{-4} W/J$)	Charge Rate ($\times 10^{-4} W/J$)
Polymer Li-ion	5.60	1.39
Ni-Cd	.03333	0.167
Ni Metal Hydride	27.78	2.78
Li-ion	3.70	2.78
LiNiMnCo	4.17	2.78

plored in [11] also considered a few other battery types, with LiNiMnCo type batteries also being used in past space missions [35]. All of these additional candidates will be competing with the Trisol-X panels and Li-Polymer batteries that were evaluated in the first study. The associated costs for each component are displayed in tables 4.2 and 4.4, with the charging and discharging rates of the batteries displayed in table 4.3.

Table 4.4: **Associated Costs for Solar Panel Alternatives**

Components	Specific Power ($\times 10^{-3} kg/W$)	Power Density ($\times 10^{-7} m^3/W$)
Tri-SolX	5.15	6.12
Spectrolab UTJ	0.621	1.03
SolAero	0.362	1.33
Endurosat	2.23	55.28
Azurspace	2.26	3.95

4.4 Manipulation of Weights

The prior studies have involved evaluating either the minimum mass or volume system. That is to mean, the tool has only exclusively considered the mass costs or the volume costs. The results are therefore the extreme ends of the trade space. There is no real reason why an aerospace designer should be limited to only considering the two extremes for their candidate systems, so a way to balance the weights, or consider the mass and volume costs without completely excluding the other one is needed. This must be done carefully, because the costs are rarely within the same order of magnitude. So, a simple shifting proportion between mass and volume costs may result in the much larger cost dominating, and the end result would not be different than exclusively considering the larger cost. The magnitude of the respective cost vector can be found and used to normalize the cost, allowing for a proportional balance between the weights similar to

$$c = p\frac{c_1}{\| c_1 \|} + (1-p)\frac{c_2}{\| c_2 \|}. \tag{4.1}$$

Using such a normalizing and proportionalizing process, it is possible to vary p from 0-1 in different steps to obtain multiple different evaluations of the problem that considers different priorities between the mass and the volume costs. Stepping across the range from 0-1 at 20 different steps should provide a clear and insightful illustration of the trade space, including the two extremes. This study will not return an optimal design, it will return several optimal designs across the trade space. The proportional constant can also be manipulated further, allowing for values greater

than 1 or less than 0. If the tool is operating correctly, it is expected that this manipulation will return dominated points, or systems that are not optimal with respect to either axis.

Chapter 5

Results

5.1 Chosen With Specified Components

All optimization is performed using Opti-Toolbox provided by Inverse Problem and interfaced through MATLAB R2016b.

5.1.1 Minimizing Battery Mass

The cost multipliers associated with the two-design decision variables is set to the determined specific power and energy of the components. When the problem is solved, it is determined that the optimal power rating of the generation module is 3.59 W, and the optimal energy capacity of the energy storage module is 3.57 Wh. Multiplying the power rating of the generation module by the specific power multiplied by two, and the energy capacity of the energy storage module by the specific energy, this corresponds to a system with 36.99 g of solar panels, and a battery with a mass

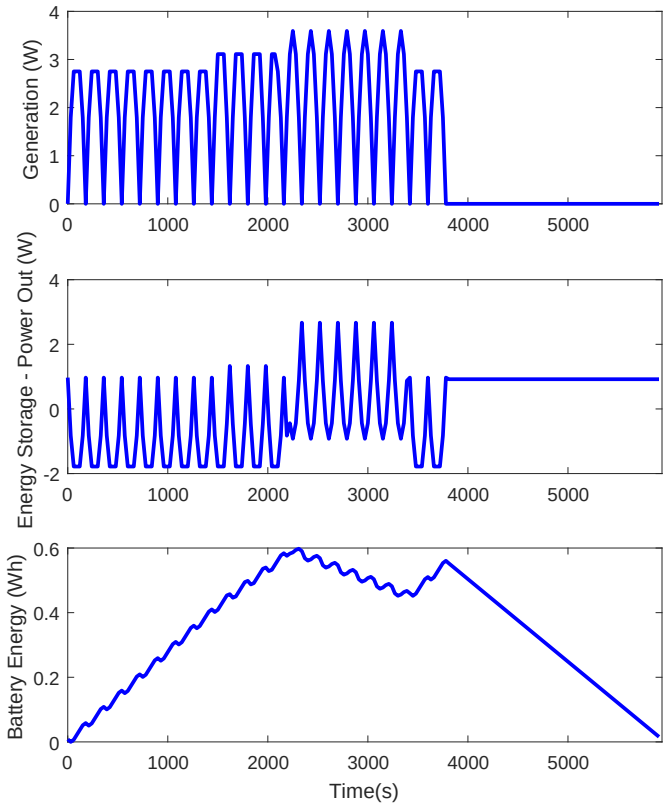

Figure 5.1: **EPS Performance, Minimum Mass Given Specified Components**

of 17.87 g. This results in a system with a total mass of 54.86 g and a total volume of 13.76 cm^3. The power system's predicted behavior is presented in figure 5.1.

5.1.2 Minimizing Battery Volume

Now, the cost multipliers of the design variables are set to the determined power and energy densities of the components. This time, solving the problem determines that the optimal power rating of the generation module is 4.41 W, the optimal energy capacity of the battery is 2.29 Wh. This results in a system with 5.39 cm^3 of solar panels, and a battery with a volume of 6.04 cm^3. The designed system is

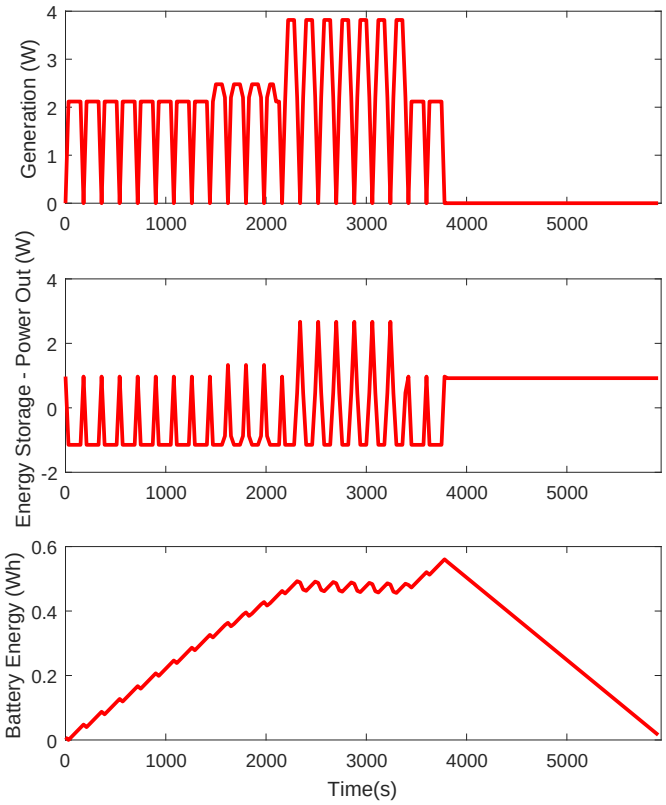

Figure 5.2: **EPS Performance, Minimum Volume Given Specified Components**

determined to have a total mass of 56.90 g, and a total volume of 11.43 cm^3 The power system's predicted behavior is presented in Figure 5.2.

Although the differences appear minor, there is a clear trade-off to observe between the two methods of minimizing the system. Analyzing the weights, minimizing the mass imposes a cost-ratio close to 1:1, while minimizing the volume imposes a cost-ratio closer to 4:1. The behaviors of both alternative systems are transposed in figure 5.3.

The most significant difference appears to be how the systems alternatively deal with the peak-load period. When minimizing the volume, the battery's impact

on the system is minimized and the system seeks to meet more of its mission load by having larger solar panels. The reverse is true when minimizing the system's mass. Before peak-load, the mass-minimized system with a larger battery requires the battery be charged to a point much larger than the alternative system, and noticeably discharges this excess over the course of the peak-load period. Both batteries of the system converge at the same capacity before entering the eclipse period, implying that the eclipse period will have no different effect on the desired control of either system.

It may appear shocking to see that neither the generation nor battery energy profiles for either system ever reach the optimal ratings determined by the solver, but this is the result of other constraints in the system. The charge and discharge rates of the battery are limited by the maximum capacity of the battery, so if a high charge rate is necessary for the system to meet load demand, the system will have a larger battery (and a larger capacity by consequence) just to make sure this is feasible. The generation profile can be explained as meeting only the demand that the battery is not already meeting, and charging the battery as little as possible to meet peak-load and eclipse energy demands. Although the generation profile rarely meets its peak possible generation, it is not necessary to do so, and the rating is raised solely to ensure that the generation module can produce enough power over time to meet the system's needs.

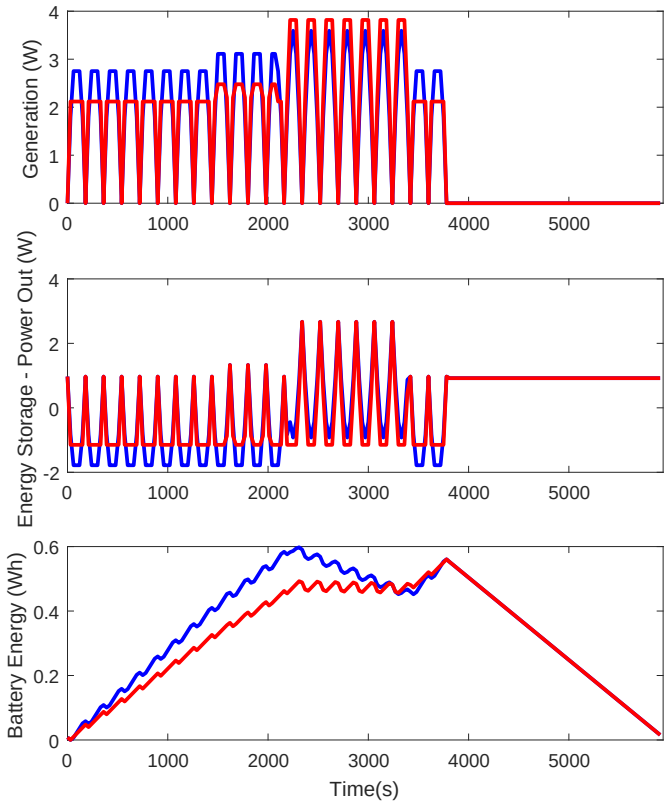

Figure 5.3: **EPS Performance, Transcribed Results Given Specified Components**

5.2 Chosen With Component Alternatives

The cost multipliers are adjusted as in the prior study to determine the minimum mass system and the minimum volume system. However, now the tool is evaluating 25 different combinations of candidate components to do it. All of the total mass costs for each candidate system evaluated by the solver are contained in table 5.1, with the behavior of the minimum mass system displayed in figure 5.4. The tool determined that the best battery is the LiNiMnCo chemistry, and the best solar panel is the SolAero panels for the purpose of minimizing system mass. It is

Table 5.1: **Minimum Mass Costs for Alternative Components (g)**

Components	Tri-SolX	Spectrolab UTJ	Solaero	Endurosat	Azurspace
Polymer Li-ion	54.81	16.96	14.51	31.05	31.27
Ni-Cd	196.88	160.01	157.90	173.17	173.39
Ni Metal Hydride	57.12	18.62	15.91	32.77	33.00
Li-ion	55.49	24.46	22.69	35.54	35.72
LiNiMnCo	46.23	14.20	12.34	25.82	26.01

determined that the optimal power rating of the generation module is 3.60 W, and the optimal energy capacity of the energy storage module is 1.78 Wh. Multiplying the power rating of the generation module by the specific power multiplied by two, and the energy capacity of the energy storage module by the specific energy, this corresponds to a system with 2.6 g of solar panels, and a battery with a mass of 9.74 g. This results in a system with a total mass of 12.34 g and a total volume of 19.98 cm^3.

All of the total volume costs for each candidate system evaluated by the solver are contained in table 5.2, with the behavior of the minimum volume system displayed in figure 5.5. The tool determined that the best battery is the Ni Metal Hydride chemistry, and the best solar panel is the Spectrolab panels for the purpose of minimizing system volume. It is determined that the optimal power rating of the generation module is 7.21 W, and the optimal energy capacity of the energy storage module is 0.93 Wh. Multiplying the power rating of the generation module by the specific power multiplied by two, and the energy capacity of the energy storage module by the specific energy, this corresponds to a system with 1.49 cm^3 of solar panels, and a battery with a volume of 3.53 cm^3. This results in a system with a total mass of 19.64 g and a total volume of 4.58 cm^3.

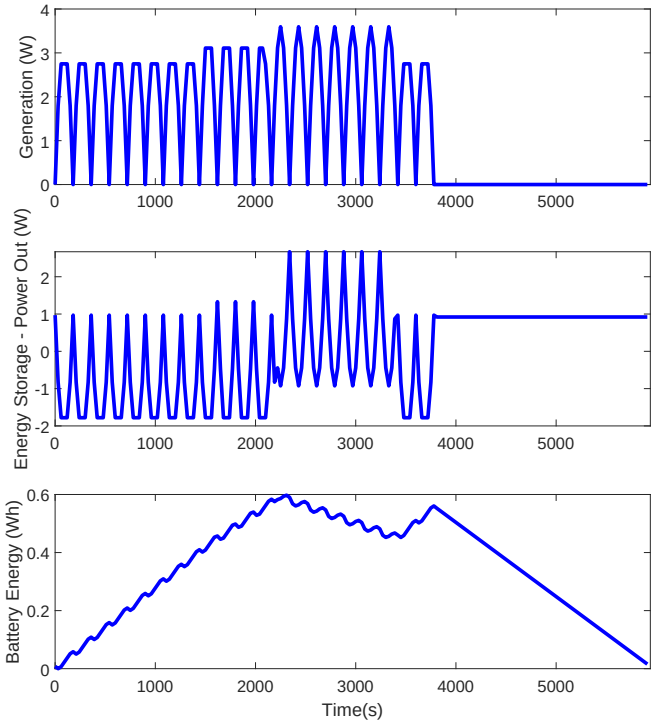

Figure 5.4: **EPS Performance, Minimum Mass Among Alternative Components**

Table 5.2: **Minimum Volume Costs for Alternative Components** (cm^3)

Components	Tri-SolX	Spectrolab UTJ	Solaero	Endurosat	Azurspace
Polymer Li-ion	11.43	6.39	6.82	48.41	9.52
Ni-Cd	89.25	85.11	85.35	129.29	87.49
Ni Metal Hydride	9.17	4.58	4.93	44.52	7.28
Li-ion	9.97	6.49	6.69	43.67	8.48
LiNiMnCo	23.42	19.76	19.98	58.76	21.86

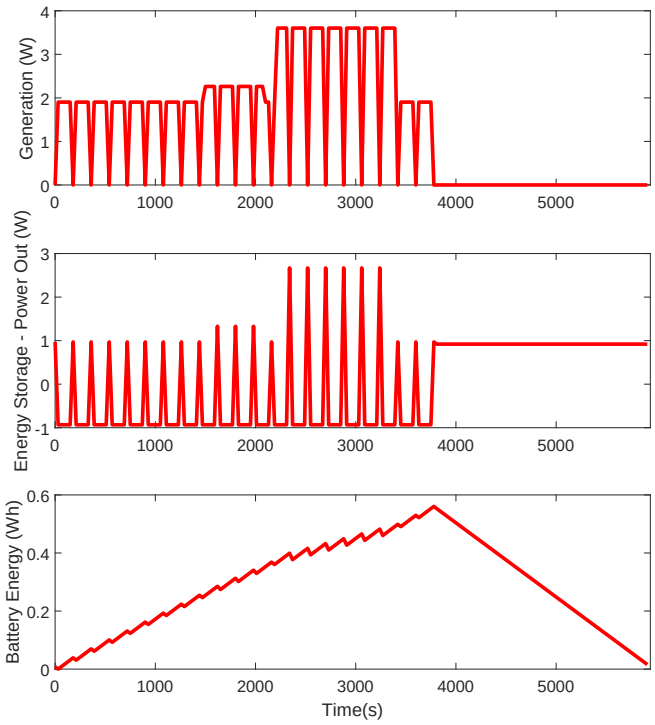

Figure 5.5: **EPS Performance, Minimum Volume Among Alternative Components**

The behaviors of both the minimum mass and minimum volume systems can be transcribed in figure 5.6 just as in the previous study to see the differences the tool is capable of exploring.

Although the behavioral differences seemed minor when comparing the minimum mass to the minimum volume systems of the same components, the differences are much more pronounced when the full range of components are available. The first thing to notice is that both systems are generally much smaller in weight and volume than the original study, but this is almost certainly due to the advances made in both solar cell and battery technology when compared to the reference configuration that was used in the original study. The next thing of note is both the minimum mass

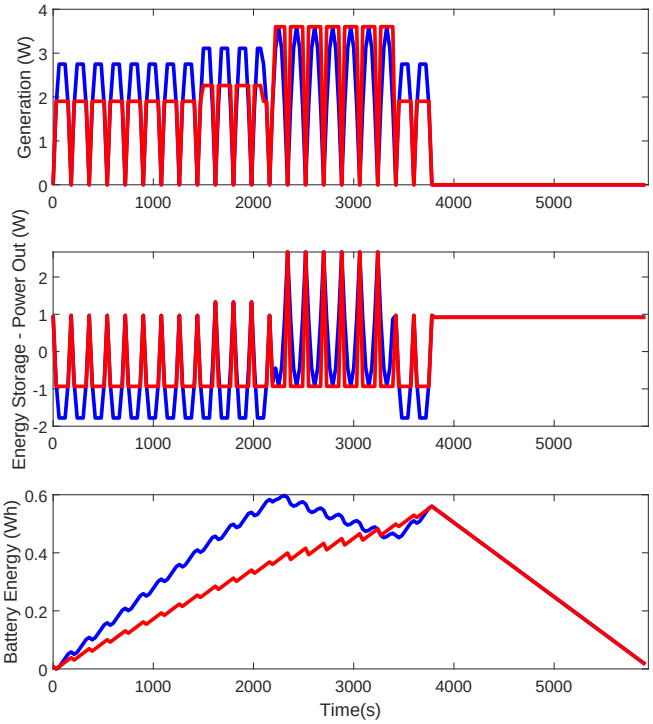

Figure 5.6: **EPS Performance, Transcribed Results Among Alternative Components**

and minimum volume systems reach the same peak power from the solar module. There is only a difference in how each system treats their peak performance. The minimum volume system needs solar cells capable of delivering a much larger peak possible power, so they can more consistently draw power at the level that both systems desire to achieve in actual performance during the high intensity load period. The minimum mass system consistently needs to draw more power from its solar module, and discharge more power from its batteries except during the high intensity load period, when both systems seem to discharge about the same amount of power. The battery of the minimum mass system seems to follow similar behavior to that of

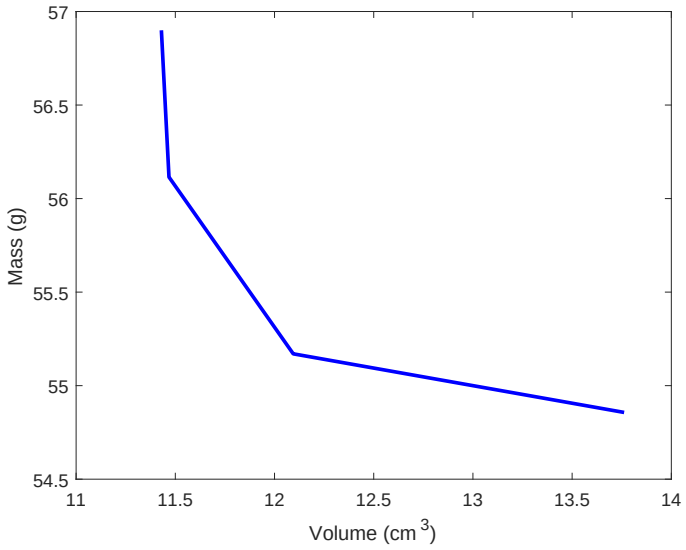

Figure 5.7: **Total System Masses vs. Total System Volumes**

the minimum mass system in the original study, while the minimum volume system never appears to achieve a net discharge of the battery until the eclipse period.

5.3 Effect of Manipulating Weights

The weights can be balanced, or varied to favor either the mass costs or the volume costs. Twenty-one different variations between the weights, including the original evaluations at both extremes considering only the mass or the volume, are evaluated with the tool. This section will display the results when several metrics of the solar and battery modules are plotted against eachother. The maximum power of the solar module will be plotted against the maximum energy capacity of the battery module, and the total mass of the systems will be plotted against the total volumes.

Observing the results from figure 5.7, the candidate systems all converge on four points despite varying the costs among many different points. The functional capabilities of the systems are displayed in figure 5.8. Looking at these graphs gives

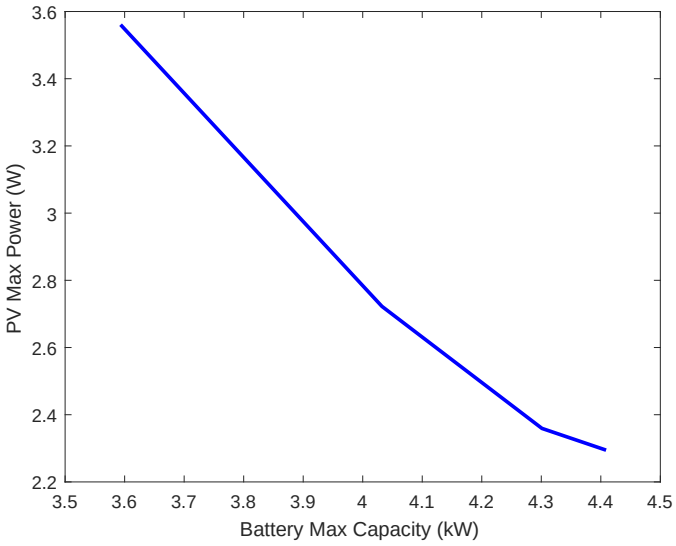

Figure 5.8: **Maximum Solar Power vs. Maximum Energy Capacity**

two different ways to observe the trade space that the aerospace designer experiences. Although the tool converges on the selected 4 points, there is no reason that an aerospace designer could not select any point on the line connecting these points depending on their needs. It is important to remember that a desired system may not be desired for the exact mission at hand that is determining the optimal systems, but for all possible missions that the system could face in the future, capitalizing on reusability and scalability of the design.

While there are intuitive reasons for not manipulating the proportional constants beyond the range between 0 and 1, there is also nothing really stopping the designer from doing it. If this happens, intuitively it is expected that the tool will return non-optimal designs, instead returning dominated points. So, a good way to measure that the tool is actually performing correctly and doing what we suspect, is to manipulate the proportional constant weighting these costs both to negative val-

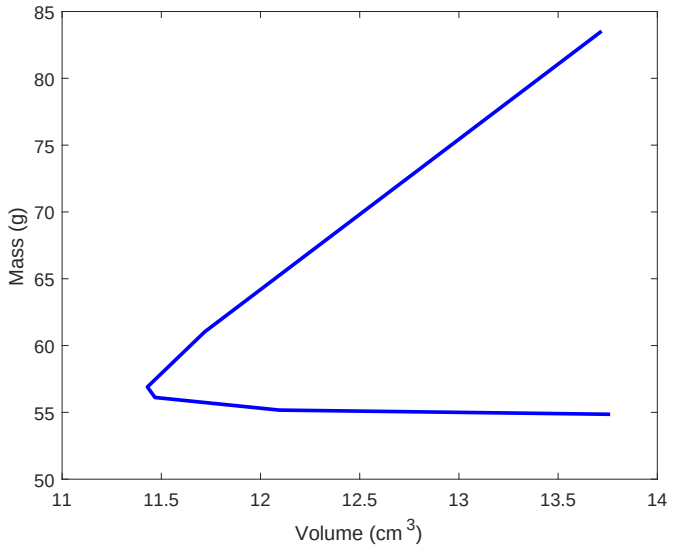

Figure 5.9: **Total System Masses vs. Total System Volumes, Negative Weights**

ues and to values greater than 1. First, the proportional constant will be distributed between -1 and 1.

It may not be clear from the graph in figure 5.9, but taking the proportional constant to negative values actually extends the left-hand tail of the curve from figure 5.7. This produces more candidate systems than the original four, but it is important to note that the additional candidate systems are dominated points. These systems give no additional benefit to either mass or volume sizing for a system that can perform the specified mission. Next, the proportional constant will be distributed from 1 to 2.

It is more clear in figure 5.11 than from the previous example, but extending the proportional constant over 1 extends the curve from figure 7 on the right-hand tail. These are also dominated points. Like the previous example, these dominated points are intuitively useless to the aerospace designer to consider for the mission at hand, but observing this effect is important because it verifies that manipulating the

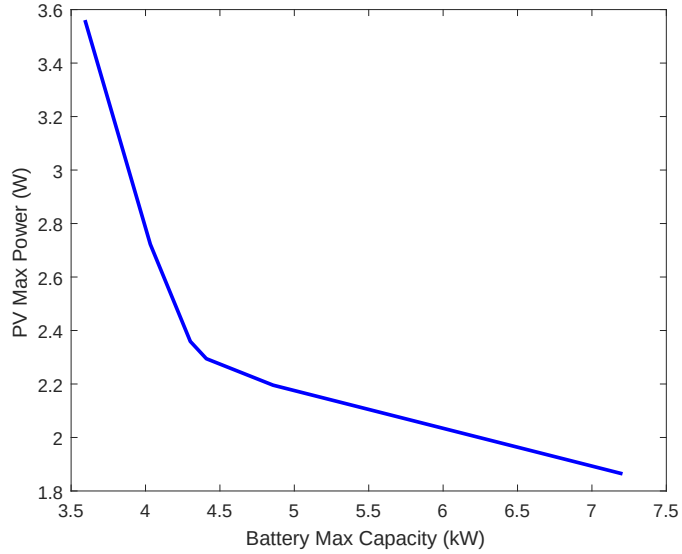

Figure 5.10: **Maximum Solar Power vs. Maximum Energy Capacity, Negative Weights**

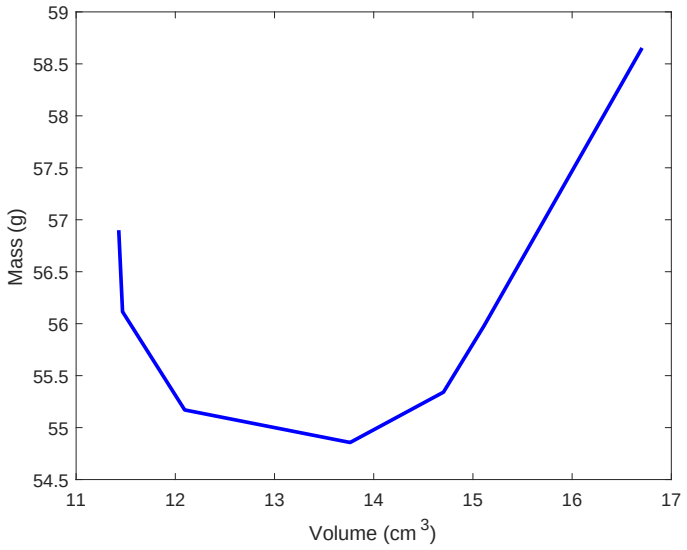

Figure 5.11: **Total System Masses vs. Total System Volumes, Weights Multiplied Over 1**

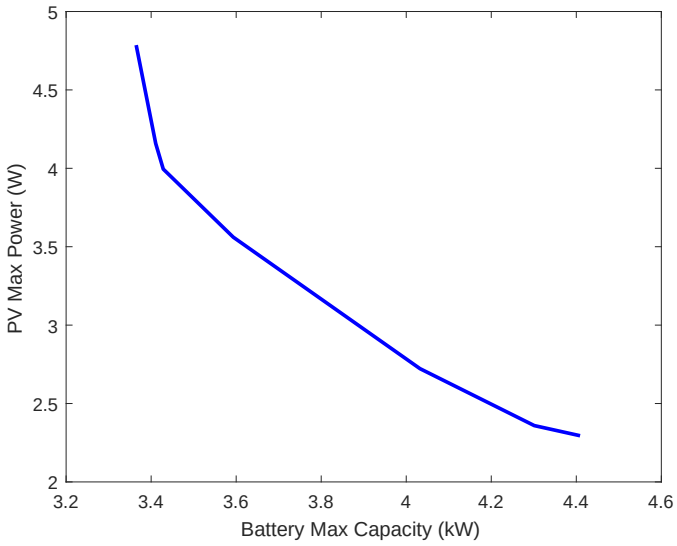

Figure 5.12: **Maximum Solar Power vs. Maximum Energy Capacity, Weights Multiplied Over 1**

weights seen by the optimizer returns expected behavior, and it is then reasonable to assume that the tool is performing as expected and not in some manner that returns some random system that is not actually optimally sized with respect to the desired metrics.

Chapter 6

Conclusions & Future Work

A mathematical design approach to the design of satellite power systems has been presented. The benefits of the modular architecture have been explained, but the tool is not limited to use in such architectures, it can in fact be applied to any kind of power system architecture as long as an appropriate system of equations exist to model the architecture. The mathematical programming approach, utilizing a multi-period system of constraints to achieve non-intuitive optimal control paths for the power system, has been explored. The design approach was exercised to solve the simple problem of finding a minimum-mass and volume system when given the specific components of a representative configuration with an expected mission, and also the more complicated problem of determining the minimum mass and volume systems when given many different component options for the satellite system. The trade space was sufficiently explored by shifting the balance between the volume and mass costs that the optimization software considers when determining the optimal configuration.

Still, a significant amount of work could still be done to improve the capability and application of the design approach. First and most obvious, the existing work that was done to linearize the I/V system breakdown should be finished to immediately deliver a more robust and useful tool in the design approach. This will make the existing tool much more realistic in terms of how the system functions in a real-world environment, and may even provide aid in trouble shooting an existing system at a component level. Second, the real-world efficiencies of the power system can be assessed and included in the calculations to provide an even more realistic view of a resulting system. The associated power conditioning devices used in association with the modules can also be included in the functional operations of the modules which will mainly just impact the efficiency metrics. The communication limitations of the system, which will be heavily influenced by the architecture, can also be accounted for when formulating the optimal energy trajectory of the system. The orbital considerations of the approach can also be improved to consider more realistic solar exposure in conjunction with the satellite's selected attitude-control system, as well as considering non-solar power alternatives for the system's power generation. All of these suggestions are just aiming to create a more robust and realistic design tool that can account for most of the real-life implications of operating a satellite power system.

In addition, the tool can also be modified slightly with a few additional constraints, to maximize the size of a power system within a given volume or mass limit. As CubeSat platforms grow to more regularly utilize 6U or 12U-sized systems, it is not uncommon for a specific set of the individual CubeSats to be dedicated to the power system of the satellite. The goal here would be to maximize the capability of the power system to best serve not only the existing load, but additional load for future

missions, perhaps capitalizing on reusability and scalability for the dedicated platforms. When considering deep-space missions, there are two competing philosophies in delivering the system to its appropriate location: a CubeSat can have propulsion capability to advance to its location, or it can be delivered via a larger "mother-ship". The existing tool can be used in the mother-ship example almost seamlessly, with only a different orbital constant and relative solar exposure depending on a target planet or body. However, a CubeSat delivering itself will need a mission with much more definition and risk assessment before an optimal energy trajectory can be accurately determined.

Bibliography

[1] M. N. Sweeting, "Modern small satellites-changing the economics of space," *Proceedings of the IEEE*, vol. 106, no. 3, pp. 343–361, March 2018.

[2] F. Ince, "A role for cubesats in responsive space," in *Proceedings of 2nd International Conference on Recent Advances in Space Technologies*, 2012.

[3] D. Baker and S. Wordenl, "The large benefits of small satellite missions," *Eos Trans. AGU*, vol. 89, no. 33, pp. 1–6, 2008.

[4] R. Hodges, N. Chahat, D. Hoppe, and J. Vacchione, "The mars cube one deployable high gain antenna," in *2016 IEEE International Symposium on Antennas and Propagation (APSURSI)*, June 2016.

[5] X. Yu and J. Zhou, "Cubesat: A candidate for the asteroid exploration in the future," in *2014 International Conference on Manipulation, Manufacturing and Measurement on the Nanoscale (3M-NANO)*, Oct 2014, pp. 261–265.

[6] T. Imken, J. Castillo-Rogez, Y. He, J. Baker, and A. Marinan, "Cubesat flight system development for enabling deep space science," in *2017 IEEE Aerospace Conference*, Mar 2017, pp. 1–14.

[7] S. Schwartz, R. Nallapu, P. Gankidi, G. Dektor, and J. Thangavelautham, "Navigating to small-bodies using small satellites," in *2018 IEEE/ION Position, Location and Navigation Symposium (PLANS)*, Apr 2018, pp. 1277–1285.

[8] A. Slavinskis, P. Janhunen, P. Toivanen, K. Muinonen, A. Penttilä, M. Granvik, T. Kohout, M. Gritsevich, A. Slavinskis, M. Pajusalu, I. Sünter, H. Ehrpais, J. Dalbins, I. Iakubivskyi, T. Eenmäe, M. Pajusalu, E. Ilbis, H. Ehrpais, K. Muinonen, M. Gritsevich, D. Mauro, J. Stupl, A. S. Rivkin, and W. F. Bottke, "Nanospacecraft fleet for multi-asteroid touring with electric solar wind sails," in *2018 IEEE Aerospace Conference*, March 2018, pp. 1–20.

[9] C. Norton, S. Pellegrino, and M. Johnson, *Small Satellites: A Revolution in Space Science*. Padadena, CA: Keck Institute for Space Studies, 2014.

[10] C. Bergsrud and S. Noghanian, "Investigating the design of a nano space solar power satellite," in *2014 USNC-URSI Radio Science Meeting (Joint with AP-S Symposium)*, July 2014, pp. 307–307.

[11] T. M. Lim, A. M. Cramer, J. E. Lumpp, and S. A. Rawashdeh, "A modular electrical power system architecture for small spacecraft," *IEEE Transactions on Aerospace and Electronic Systems*, vol. 54, no. 4, pp. 1832–1849, Aug 2018.

[12] T. A. Trapp, "Shipboard integrated engineering plant survivable network optimization," Ph.D. dissertation, Massachusetts Institute of Technology, 2015.

[13] Z. Chen, Z. Wang, C. Wang, and M. Chen, "Input ripple current characteristics of aviation static inverter," *IEEE Transactions on Aerospace and Electronic Systems*, vol. 49, no. 3, pp. 1667–1676, 2013.

[14] F. Belloni, P. Maranesi, and M. Riva, "Dc/dc converter for the international space station," *IEEE Transactions on Aerospace and Electronic Systems*, vol. 46, no. 2, pp. 623–634, May 2010.

[15] S. D. Sudhoff, S. F. Glover, P. T. Lamm, D. H. Schmucker, and D. E. Delisle, "Admittance space stability analysis of power electronic systems," *IEEE Transactions on Aerospace and Electronic Systems*, vol. 36, no. 3, pp. 965–973, July 2000.

[16] A. Griffo and J. Wang, "Large signal stability analysis of 'more electric' aircraft power systems with constant power loads," *IEEE Transactions on Aerospace and Electronic Systems*, vol. 48, no. 1, pp. 477–489, Jan 2012.

[17] J. R. Wetz and W. J. Larson, *Space Mission Analysis and Design.* New York, NY: Springer, 1999.

[18] D. Kaslow, B. Ayres, P. T. Cahill, L. Hart, and R. Yntema, "Developing a cubesat model-based system engineering (mbse) reference model — interim status 3," in *2017 IEEE Aerospace Conference*, March 2017, pp. 1–15.

[19] A. M. Mohamed, F. E. H. Amer, R. M. Mostafa, and A. A. H. Mahmoud, "Trade-off analysis of low earth orbit spacecraft power supply system by genetic algorithm," in *2016 IEEE Aerospace Conference*, March 2016, pp. 1–13.

[20] S. Dahbi, A. Aziz, S. Zouggar, N. Benazzi, H. Zahboune, and M. Elhafyani, "Design and sizing of electrical power source for a nanosatellite using photovoltaic cells," in *2015 3rd International Renewable and Sustainable Energy Conference (IRSEC)*, Dec 2015, pp. 1–6.

[21] S. Notani and S. Bhattacharya, "Flexible electrical power system controller design and battery integration for 1u to 12u cubesats," in *2011 IEEE Energy Conversion Congress and Exposition*, Sep 2011, pp. 3633–3640.

[22] M. Sivapalanirajan, J. Kamala, and B. Umamaheswari, "Power system design and parameter monitoiring for 2u cubesat," in *2014 International Conference on Science Engineering and Management Research (ICSEMR)*, Nov 2014, pp. 1–7.

[23] A. Dono, L. Plice, J. Mueting, T. Conn, and M. Ho, "Propulsion trade studies for spacecraft swarm mission design," in *2018 IEEE Aerospace Conference*, Mar 2018, pp. 1–12.

[24] S. Janson, "25 years of small satellites," in *25th Annual Conference on Small Satellites*, Aug 2011, pp. 1–13.

[25] A. Toorian, K. Diaz, and S. Lee, "The cubesat approach to space access," in *2008 IEEE Aerospace Conference*, March 2008, pp. 1–14.

[26] S. Kulkarni, S. Bangade, M. Khadse, D. Waghulde, P. Aher, K. Gaikwad, and S. Thakurdesai, "Design and optimization of the on board dc/dc converters of swayam satellite," in *2014 IEEE International Conference on Power Electronics, Drives and Energy Systems (PEDES)*, Dec 2014, pp. 1–6.

[27] A. I. Aravanis, B. Shankar M. R., P. Arapoglou, G. Danoy, P. G. Cottis, and B. Ottersten, "Power allocation in multibeam satellite systems: A two-stage multi-objective optimization," *IEEE Transactions on Wireless Communications*, vol. 14, no. 6, pp. 3171–3182, June 2015.

[28] A. F.III, A. Cramer, and Y. Zhang, "Market-based control as a paradigm for power system control," in *Advanced Machinery Technology Symposium 2018.*, Mar 2018, pp. 85–92.

[29] S. Ibrahim, A. Cramer, and Y. Liao, "Integrated distribution system optimization using a chance-constrained formulation," in *2017 North American Power Symposium (NAPS)*, Sep 2017, pp. 1–6.

[30] F. Tamp and P. Ciufo, "A sensitivity analysis toolkit for the simplification of mv distribution network voltage management," *IEEE Transactions on Smart Grid*, vol. 5, no. 2, pp. 559–568, Jan 2014.

[31] A. Umana and A. Meliopoulos, "The extraction of photovoltaic module parameters using fibonacci and steepest descent methods," in *2015 North American Power Symposium (NAPS)*, Oct 2015, pp. 1–6.

[32] H. R.-E. . F. B. . M.-Y. Chow, "Modeling and online parameter identification of li-polymer battery cells for soc estimation," in *2012 IEEE International Symposium on Industrial Electronics*, May 2012, pp. 1336–1341.

[33] D. Erb, "Evaluating the effectiveness of peak power tracking technologies for solar arrays on small spacecraft," Ph.D. dissertation, University of Kentucky, 2011.

[34] T. A. Rouk, S. Kim, and C. Mengu, "Design and implementation of electrical double layer capacitor (edlc) based 1u cubesat electrical power system (eps)," in *36th ISAS Space Energy Symposium*, Feb 2017.

[35] K. B. Chin, E. J. Brandon, R. V. Bugga, M. C. Smart, S. C. Jones, F. C. Krause, W. C. West, and G. G. Bolotin, "Energy storage technologies for small satellite applications," *Proceedings of the IEEE*, vol. 106, no. 3, pp. 419–428, March 2018.

Vita

Author's Name
Allen W. Flath III

Education
Bachelor of Science in Electrical Engineering from the University of Kentucky, 2017. Magna Cum Laude

Publications
A. W. Flath, A. M. Cramer and X. Liu, "Control system modeling in early-stage simulation for cyber vulnerability assessment," 2017 IEEE Electric Ship Technologies Symposium (ESTS), Arlington, VA, 2017, pp. 9-15.

A. W. Flath, A. M. Cramer and Y. Zhang, "Market-based control as a paradigm for power system control," 2018 ASNE Advanced Machinery Technology Symposium (AMTS), Pittsburgh, PA, 2018, pp 1-6.

A. W. Flath, A. M. Cramer and J. E. Lumpp, "Mathematical programming based approach to modular electric power system design," 2019 IEEE Aerospace, Big Sky, MT, 2019, pp 1-8.